NASA/TM—2010-216252 AIAA–2010–0810



# *Orion* Active Thermal Control System Dynamic Modeling Using Simulink/MATLAB

*Xiao-Yen J. Wang and James Yuko*
*Glenn Research Center, Cleveland, Ohio*

May 2010

# NASA STI Program . . . in Profile

Since its founding, NASA has been dedicated to the advancement of aeronautics and space science. The NASA Scientific and Technical Information (STI) program plays a key part in helping NASA maintain this important role.

The NASA STI Program operates under the auspices of the Agency Chief Information Officer. It collects, organizes, provides for archiving, and disseminates NASA's STI. The NASA STI program provides access to the NASA Aeronautics and Space Database and its public interface, the NASA Technical Reports Server, thus providing one of the largest collections of aeronautical and space science STI in the world. Results are published in both non-NASA channels and by NASA in the NASA STI Report Series, which includes the following report types:

- TECHNICAL PUBLICATION. Reports of completed research or a major significant phase of research that present the results of NASA programs and include extensive data or theoretical analysis. Includes compilations of significant scientific and technical data and information deemed to be of continuing reference value. NASA counterpart of peer-reviewed formal professional papers but has less stringent limitations on manuscript length and extent of graphic presentations.

- TECHNICAL MEMORANDUM. Scientific and technical findings that are preliminary or of specialized interest, e.g., quick release reports, working papers, and bibliographies that contain minimal annotation. Does not contain extensive analysis.

- CONTRACTOR REPORT. Scientific and technical findings by NASA-sponsored contractors and grantees.

- CONFERENCE PUBLICATION. Collected papers from scientific and technical conferences, symposia, seminars, or other meetings sponsored or cosponsored by NASA.

- SPECIAL PUBLICATION. Scientific, technical, or historical information from NASA programs, projects, and missions, often concerned with subjects having substantial public interest.

- TECHNICAL TRANSLATION. English-language translations of foreign scientific and technical material pertinent to NASA's mission.

Specialized services also include creating custom thesauri, building customized databases, organizing and publishing research results.

For more information about the NASA STI program, see the following:

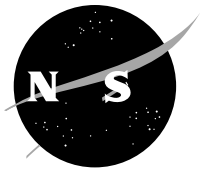
- Access the NASA STI program home page at *http://www.sti.nasa.gov*

- E-mail your question via the Internet to *help@sti.nasa.gov*

- Fax your question to the NASA STI Help Desk at 443–757–5803

- Telephone the NASA STI Help Desk at 443–757–5802

- Write to:
  NASA Center for AeroSpace Information (CASI)
  7115 Standard Drive
  Hanover, MD 21076–1320


N
S

| | |
|---|---|
| $m_c$ | mass of cold fluid in heat exchanger |
| $m_{f,1}$, $m_{f,2}$ | mass of fluid in the two loops |
| $m_{HX}$ | mass of heat exchanger |
| $m_h$ | mass of hot fluid in heat exchanger |
| $m_i$ | mass of the three sections on the panel (where $i$ = 1, 2, 3) |
| $\dot{m}_c$ | mass flow rate of cold fluid in heat exchanger |
| $\dot{m}_h$ | mass flow rate of hot fluid in heat exchanger |
| $\dot{m}_1$, $\dot{m}_2$ | mass flow rates of the two loops |
| Pr | Prandtl number |
| $Q_a$ | total heat flux on the radiator panel from solar, albedo, and planetshine |
| $Q_{\text{hot2wall}}$ | heat flux from the hot stream to the wall |
| $Q_{\text{wall2cold}}$ | heat flux from wall to the cold stream |
| $q_1$, $q_2$ | heat flux |
| $R_1$, $R'_1$ | convection resistances between fluid and channel wall |
| $R_2$, $R'_2$ | conduction resistances through panel thickness |
| $R_3$, $R_4$ | conduction resistances along panel |
| $R_5$, $R_6$, $R_7$ | adiation resistances between panel surface and ambient environment |
| $T_a$ | equivalent ambient or sink temperature |
| $T_{c,e}$ | cold-stream exit temperature |
| $T_{c,i}$ | cold-stream inlet temperature |
| $T_{h,e}$ | hot-stream exit temperature |
| $T_{h,i}$ | hot-stream inlet temperature |
| $T_{\text{wall}}$ | wall temperature |
| $T_{i,1}$, $T_{i,2}$ | fluid inlet temperatures for the two fluid loops |
| $T_{p,a}$ | temperature at panel between the two fluid channels |
| $T_{p,1}$, $T_{p,2}$ | temperatures at panel right above the fluid channel |
| $T_{w,1}$ $T_{w,2}$ | wall temperatures of fluid channel |
| Re | Reynolds number |
| $T_{1,i}$, $T_{2,i}$, | fluid inlet temperatures |
| $T_{1,o}$, $T_{2,o}$ | fluid exit temperatures |
| $t$ | time |
| ε | surface emissivity |
| σ | Stefan-Boltzmann constant |
| β | the angle between the solar vector and the orbit plane |

# Mathematical Models of the Heat Exchanger and Radiator

## One-Dimensional Transient Model for the Heat Exchanger

The heat exchanger considered here is a typical compact HX with plain-fin surfaces as shown in Figure 2. It is in a counter-flow arrangement.

The inlet and exit temperatures are $T_{h,i}$ and $T_{h,e}$, respectively, for the hot-stream, $T_{c,i}$ and $T_{c,e.}$ for the cold-stream. Given the inlet temperature of both sides, $T_{h,e}$, $T_{c,e}$, and the wall temperature $T_{\text{wall}}$ can be solved through the following ordinary differential equations:

$$\frac{dT_{h,e}}{dt} = \left(-Q_{\text{hot2wall}} + \dot{m}_h c_{p,h}\left(T_{h,i} - T_{h,e}\right)\right)/\left(m_h c_{p,h}\right)$$
$$\frac{dT_{c,e}}{dt} = \left(Q_{\text{wall2cold}} + \dot{m}_c c_{p,c}\left(T_{c,i} - T_{c,e}\right)\right)/\left(m_c c_{p,c}\right)$$
$$\frac{dT_{\text{wall}}}{dt} = \left(Q_{\text{hot2wall}} - Q_{\text{wall2cold}}\right)/\left(m_{HX} c_{p,HX}\right)$$

where

$$Q_{\text{hot2wall}} = hA_{\text{hot}}\left(\left(T_{h,i} + T_{h,e}\right)/2 - T_{\text{wall}}\right)$$
$$Q_{\text{wall2cold}} = hA_{\text{cold}}\left(T_{\text{wall}} - \left(T_{c,i} + T_{c,e}\right)/2\right)$$

$t$ is time; $Q_{\text{hot2wall}}$ and $Q_{\text{wall2cold}}$ are the heat flux from the hot stream to the wall and from the wall to the cold stream; $hA_{\text{hot}}$ and $hA_{\text{cold}}$ are the heat transfer rates for the hot and cold fluids; $m_h$, $m_c$, and $m_{HX}$ are the masses of the hot fluid, cold fluid, and the heat exchanger itself; $c_{p,h}$, $c_{p,c}$, and $c_{p,HX}$ are the specific heats of the hot fluid, cold fluid, and heat exchanger; and $\dot{m}_h$ and $\dot{m}_c$ are the mass flow rates of the hot and cold fluids, respectively.

## One-Dimensional Transient Model of the Radiator Panel With Fluid Loops

The radiator panel has a thin surface with fluid channels attached at its interior surface. The interior surface is covered by multilayer insulation (MLI) blankets. The exterior surface is coated with material that has high emissivity. The fluid loop will come into the header and split the flow through a number of channels along the panel. For the two-loop (A and B) flow configuration, the channel will flow alternately along fluid loops A and B. The flow condition in the two loops can be different. A cross section of the radiator panel in the flow direction (sketched in Fig. 3) shows the two neighboring fluid channels denoted as loop A and loop B. On the exterior surface of the radiator panel, $T_{p,1}$ and $T_{p,2}$ are the temperatures at the panel right above the fluid channel, $T_{p,a}$ is the temperature at the panel between the two fluid channels, and $T_{w,1}$ and $T_{w,2}$ are the wall temperatures of the fluid channel.

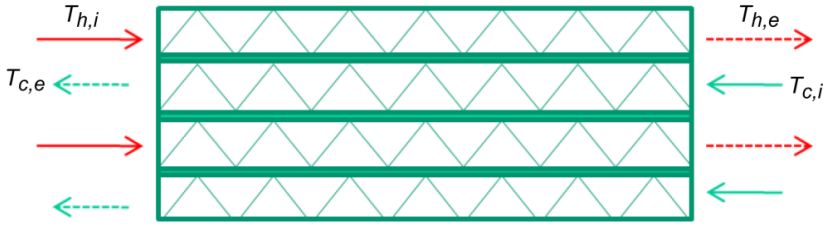



Figure 2.—Counter-flow heat exchanger (HX).

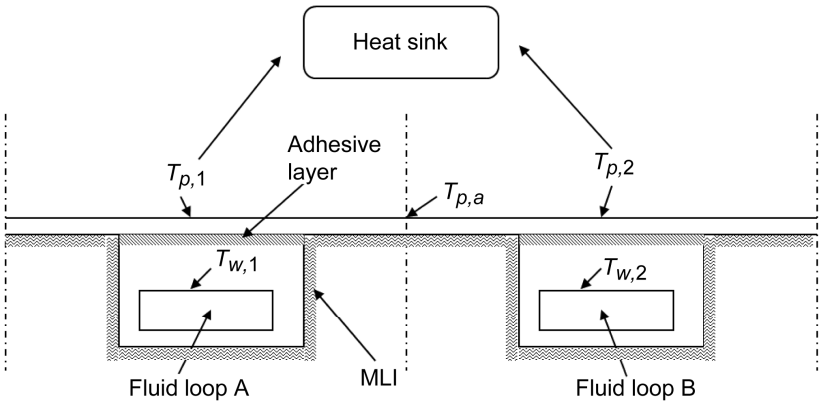



Figure 3.—Section of radiator panel showing the two fluid loops: A and B. MLI, multilayer insulation.

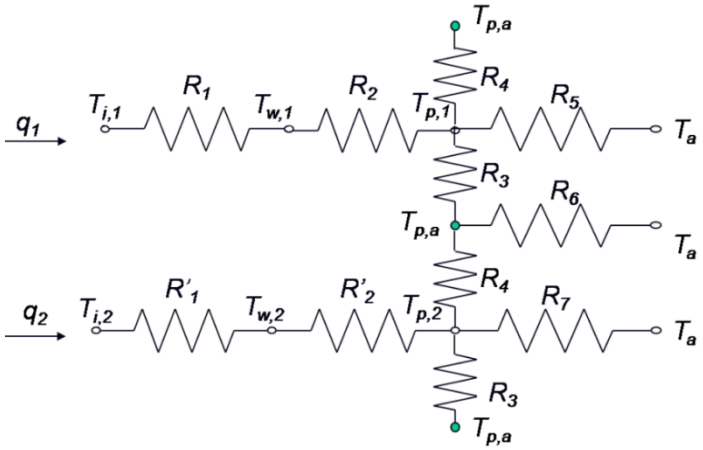



Figure 4.—Thermal circuit for radiator panel.

The corresponding thermal circuit is plotted in Figure 4. $R_1$ and $R'_1$ are the convection resistances between the fluid and the channel wall; $R_2$ and $R'_2$ are the conduction resistances through the panel and the adhesive layer thickness; $R_3$ and $R_4$ are the conduction resistances along the panel; $R_5$, $R_6$, and $R_7$ are the radiation resistances between the panel surface and the ambient environment; $T_{i,1}$ and $T_{i,2}$ are the fluid inlet temperatures for the two fluid loops (assumed to be given); and $T_a$ is the equivalent ambient or radiation sink temperature. In space, the radiator panel is exposed to the Sun, the planet, and deep space. For this model, $Q_a$ is the total heat flux from the Sun, albedo, and planetshine on the radiator panel. It is assumed that $Q_a = A_p \sigma \varepsilon T_a^4$, with $A_p$ being the radiator panel area, $\sigma$ the Stefan-Boltzmann Constant, and $\varepsilon$ the surface emissivity. Then the radiation sink temperature $T_a$ can be used to represent the ambient condition. For all cases, the sink temperatures were computed using a separate Thermal Desktop model and were used as input to the Simulink model. The Thermal Desktop model performed full three-dimensional transient analysis for orbit heating on all the radiator panels and averaged the results over the entire panel to generate one sink temperature for each panel. Radiation between the large structures, such as solar arrays and radiator panels, is included in the model.

In the model, $m_i$ and $A_{p,i}$ (where $i$ = 1, 2, 3) denote the mass and the area of the three sections of the panel; $c_{p,r}$ and $c_{p,f}$ are the specific heats of the radiator panel and the fluid, $m_{f,1}$ and $m_{f,2}$ are the masses of the fluid in the two loops, and $\dot{m}_1$ and $\dot{m}_2$ are the mass flow rates of the two loops. The equations for

solving the three panel wall temperatures, $T_{p,1}$, $T_{p,2}$, and $T_{p,a}$, and two fluid exit temperatures, $T_{1,o}$ and $T_{2,o}$, follow:

$$m_1 c_{p,r} \frac{\partial T_{p,1}}{\partial t} = q_1 - \frac{2\left(T_{p,1} - T_{p,a}\right)}{R_3} - A_{p,1}\sigma\varepsilon\left(T_{p,1}^4 - T_a^4\right)$$

$$m_2 c_{p,r} \frac{\partial T_{p,2}}{\partial t} = q_2 - \frac{2\left(T_{p,2} - T_{p,a}\right)}{R_4} - A_{p,2}\sigma\varepsilon\left(T_{p,2}^4 - T_a^4\right)$$

$$m_3 c_{p,r} \frac{\partial T_{p,a}}{\partial t} = \frac{2\left(T_{p,1} - T_{p,a}\right)}{R_3} + \frac{2\left(T_{p,2} - T_{p,a}\right)}{R_4} - A_{p,3}\sigma\varepsilon\left(T_{p,a}^4 - T_a^4\right)$$

$$m_{f,1} c_{p,f} \frac{\partial T_{1,o}}{\partial t} = -q_1 + \dot{m}_1 c_{p,f}\left(T_{1,i} - T_{1,o}\right)$$

$$m_{f,2} c_{p,f} \frac{\partial T_{2,o}}{\partial t} = -q_2 + \dot{m}_2 c_{p,f}\left(T_{2,i} - T_{2,o}\right)$$

where

$$q_1 = hA\left(\left(T_{1,i} + T_{1,o}\right)/2 - T_{p,1}\right)$$
$$q_2 = hA\left(\left(T_{2,i} + T_{2,o}\right)/2 - T_{p,2}\right)$$

with

$hA = 7.54\ kA/Dh$ for $\mathrm{Re} \le 2000$

$hA = 0.023 * \mathrm{Re}^{0.8}\mathrm{Pr}^{0.333}\ kA/Dh$ for $\mathrm{Re} > 2000$ (Colburn equation)

where $q_1$ and $q_2$ are the heat flux from the stream to the panel, $A$ is the heat transfer area, Re is the Reynolds number, Pr is the Prandtl number, $k$ is the thermal conductivity of the fluid, and $Dh$ is the hydraulic diameter of the fluid channel.

## Validation of the Radiator Mathematical Models

Since the radiator will be one of the major components in the ATCS, the transient model must be validated. The radiator studied here is a cylindrical surface divided into eight panels. Two flow loops go through all seven panels in series as shown in Figure 5. The eighth panel does not have flow channels attached to it and remains a panel to close out the structure. Four cases were used for the validation and described as follows.

The first case was low Earth orbit (LEO) hot case at an altitude of 230 km, β = 56°, aft to the Sun, with pitch/yaw/roll/ (P/Y/R) angles of 5°/–5°/0°. The Thermal Desktop results of the non-dimensional sink temperature and the equivalent heat flux from the environment were plotted in Figures 6(a) and 6(b) for one orbit cycle time of 1.5 hr. With a given mass flow rate and the inlet fluid temperature, the computed results of the non-dimensional fluid temperature at the exit of the last panel and the total heat rejection were plotted in Figures 6(c) and 6(d) in comparison with the corresponding Thermal Desktop (TD) results. The maximum difference between the current result and the TD result was less than 2 to 3 percent in the fluid temperature and total heat rejection.

The second case was LEO hot case at the altitude of 230 km, β = 75°, nose forward, with P/Y/R angles of 0°/0°/0°. The environmental heat fluxes were similar to the first case except that the average seven-panel heat flux had abrupt changes for the first case. The corresponding results were plotted in Figure 7 showing a similar agreement as in the first case.

The third case was lunar transit, aft to the Sun, with P/Y/R angles of 0°/0°/0°. It was a cold steady-state case. The non-dimensional fluid exit temperature maximum difference between the two solution sets was within 1.5 percent as shown in Figure 8.

The fourth case was low lunar orbit (LLO) hot case at an altitude of 90 km, β = 0°, nose forward, with P/Y/R angles of 0°/0°/0°. The non-dimensional sink temperautre and the equivalent orbit heating flux were plotted in Figure 9 for an orbit time of 2 hr. It can be seen that the environment is more severe and could be extremely hot and cold. The computed fluid temperature and heat rejection results show similar trend as shown in TD results.

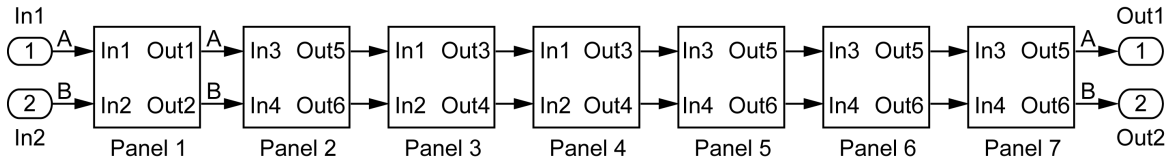



Figure 5.—Seven-panel radiator with two fluid loops.

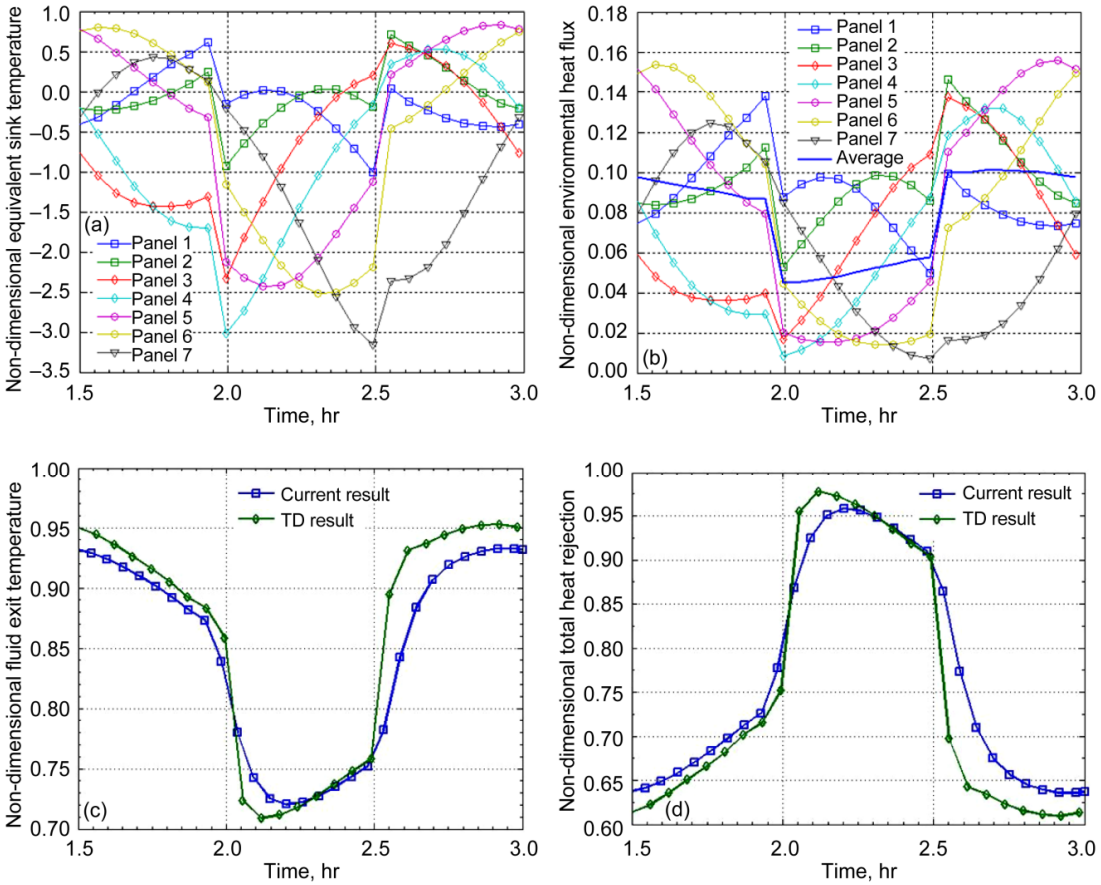



Figure 6.—Results for case 1: Low Earth orbit (LEO) aft-to-Sun hot. (a) Sink temperature. (b) Equivalent orbit heating. (c) Fluid exit temperature. (d) Total heat rejection.

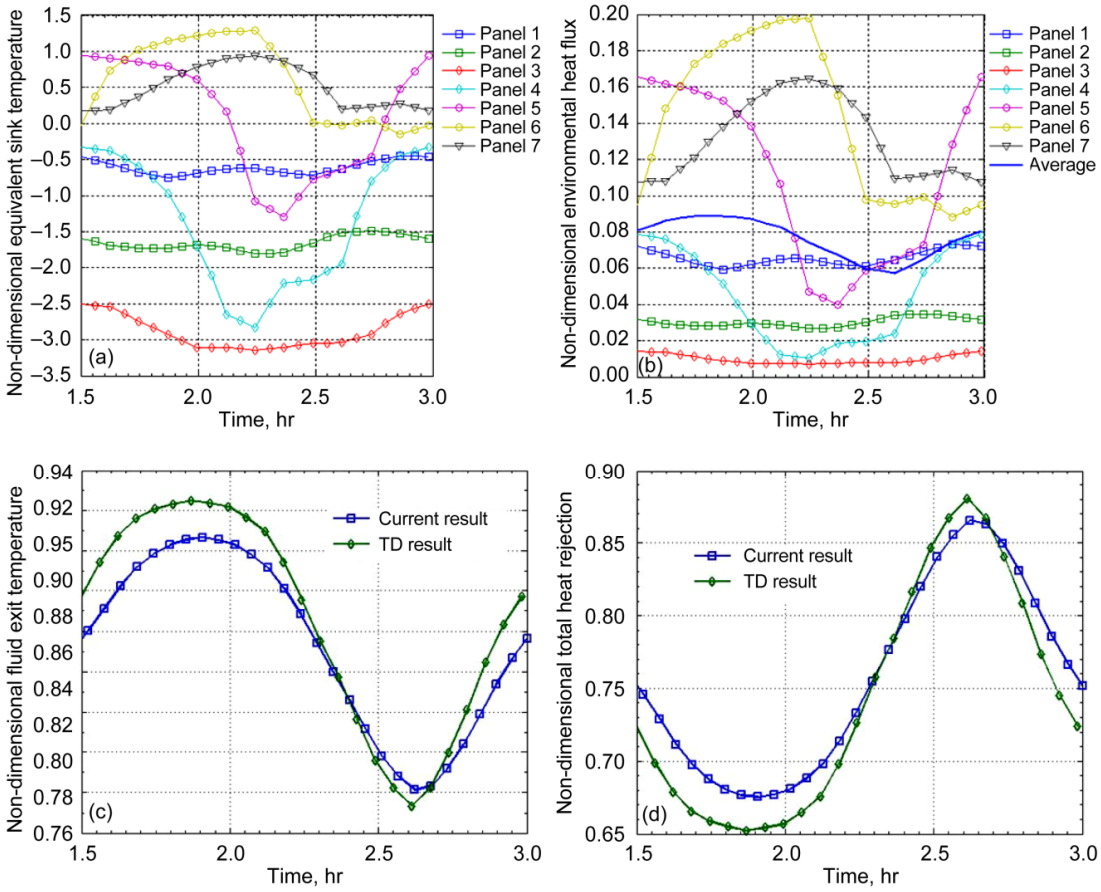



Figure 7.—Results for case 2: LEO nose-forward hot. (a) Sink temperature. (b) Equivalent orbit heating. (c) Fluid exit temperature. (d) Total heat rejection.

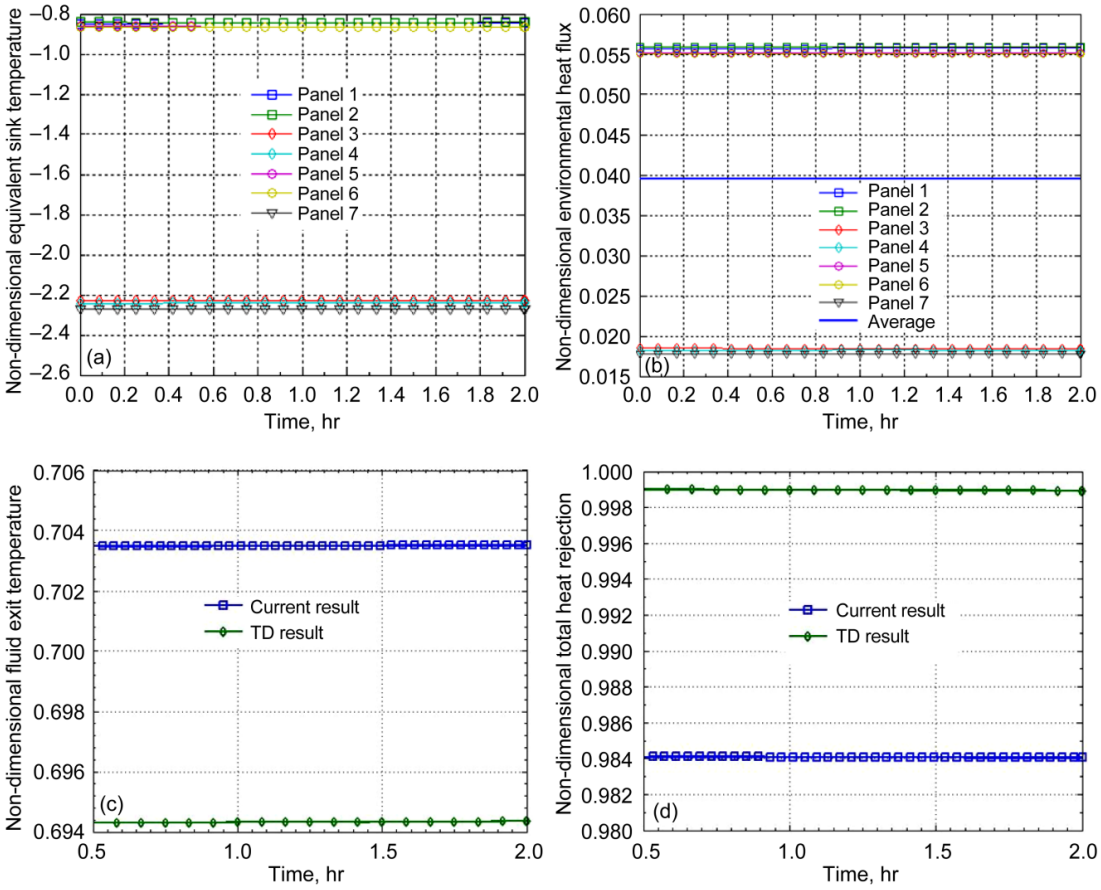



Figure 8.—Results for case 3: Lunar-transit, aft-to-Sun cold. (a) Sink temperature. (b) Equivalent orbit heating. (c) Fluid exit temperature. (d) Total heat rejection.

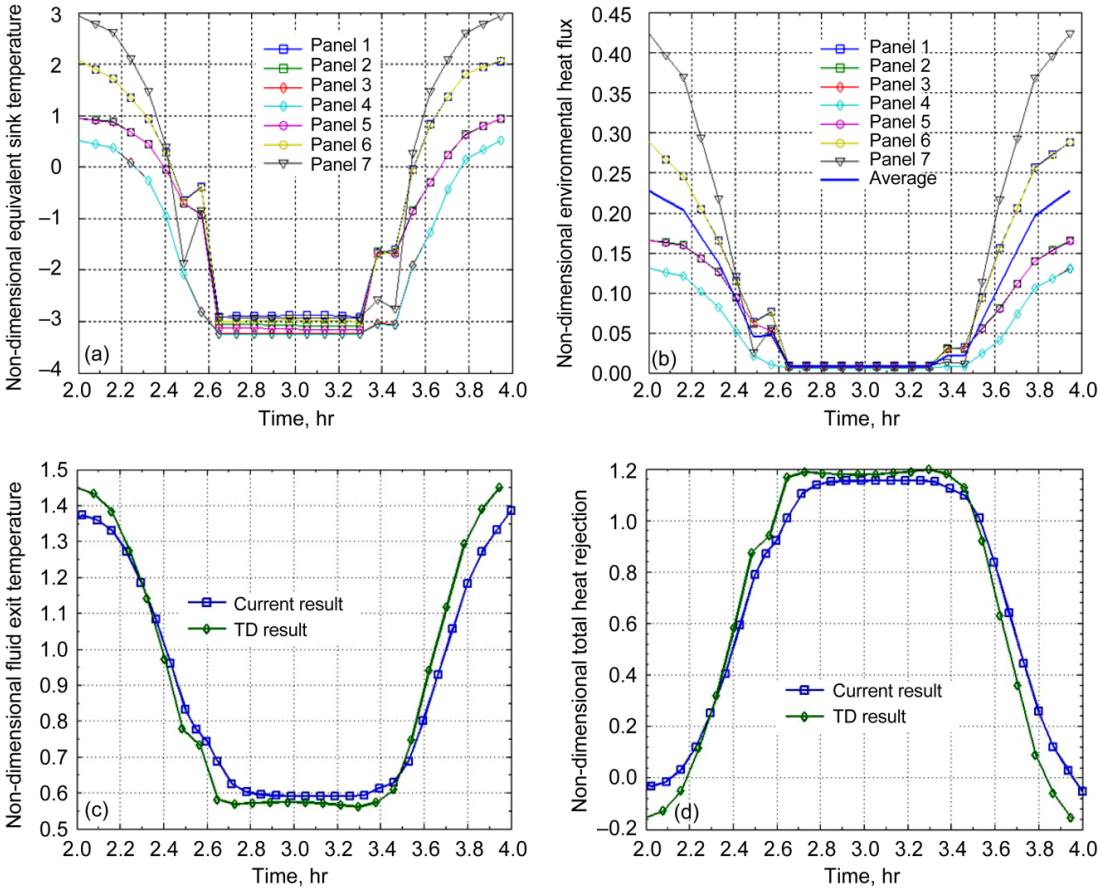



Figure 9.—Results for case 4: Low lunar orbit (LLO), nose-forward hot. (a) Sink temperature. (b) Equivalent orbit heating. (c) Fluid exit temperature. (d) Total heat rejection.

In summary, the one-dimensional transient model results agree reasonably well with the three-dimensional Thermal Desktop model results for all four orbits. It can be concluded that the one-dimensional transient model for the radiator can capture the radiator performance accurately.

## Active Thermal Control System Model Validation

The ATCS for the ISS mission will have an eight-panel radiator with no PCM HX, whereas the ATCS for the lunar mission will have a seven-panel radiator with a PCM HX since the LLO environment is generally much worse than that in LEO.

Three orbit cases were used for validation. The first case was for an ISS mission, LEO aft-to-Sun hot at an altitude of 230 km, $\beta = 75^\circ$, P/Y/R angles of 5º/–5º/0º, and a power load of 4683 W; The second case was for a lunar mission, LLO nose-nadir hot at an altitude of 75 km, $\beta = 0^\circ$, P/Y/R angles of –20º/20º/0º, and a power load of 2571 W; and the third case also was for a lunar mission, LLO aft-to-Sun cold at an altitude of 400 km, $\beta = 90^\circ$, P/Y/R angles of 0º/0º/0º, and a power load of 1725 W.

Four sets of solution were compared: (1) current Simulink model results, (2) an independent Simulink model results, (3) SINDA/FLUINT model results, and (4) FloCAD model results. The modeling details of the other three models were not available. The current Simulink model uses the same heat transfer characteristic of all HXs in the ATCS as those used in other three models. The SINDA/FLUINT model has a full three-dimensional radiator model. All models use a similar mathematical approach. Simulink is a commercial tool for modeling, simulating and analyzing multidomain dynamic systems. SINDA/FLUINT is a comprehensive finite-difference, lumped parameter (circuit or network analogy) tool for heat transfer design analysis and fluid flow analysis in complex systems. FloCAD is a Thermal Desktop module that allows a user to develop and integrate both fluid and thermal systems within a CAD based environment. Like Thermal Desktop, FloCAD is a graphical user interface for SINDA/FLUINT.

In the current Simulink/MATLAB model, 20 mesh points are used in the flow direction for the IFHX, 30 mesh points are used in the flow direction for the Regen HX, and two mesh points are used in the flow direction for the sublimator and PCM HX. The heat transfer rate for the IFHX, Regen HX, sublimator, and PCM HX were referred to in Reference 5. For the cabin HX and cold plate for the CM and SM sides, a constant heat load based on the power load was imposed. For the radiator, two mesh points were used for each panel, and all panels were modeled.

The solver used in the Simulink model is ODE45(Dormand-Prince) with a variable time step. The maximum $\Delta t$ was 0.5 s, otherwise the result would have diverged. The model took approximately 20 min to simulate a three-orbit (4.5-hr) run.

For each case, the non-dimensional fluid temperatures on the CM side (including the cabin inlet, SM cold plate inlet, IFHX inlet, PCM inlet, and sublimator inlet) and the fluid temperatures on the SM side (including the IFHX cold side exit, Regen HX exit, and radiator exit temperature) were plotted. The IFHX bypass flow fraction and Regen HX bypass flow fraction also were plotted. Four sets of solution were plotted side by side for comparison.

Figure 10 shows plots of the non-dimensional Thermal Desktop results of the sink temperature for the eight radiator panels for the LEO aft-to-Sun hot case. Figures 11 and 12 show plots of the all four model results for both the CM and SM sides. The non-dimensional sink temperature changed from –1.70 to 0.55, showing a mild orbit heating environment. All four model results show similar trends for the IFHX bypass flow changes and a similar on-and-off pattern for the sublimator. Some oscillations exist in the FloCAD model because of the algorithm for turning the sublimator water on and off. On the SM side, all four models show that the Regen HX is not used.

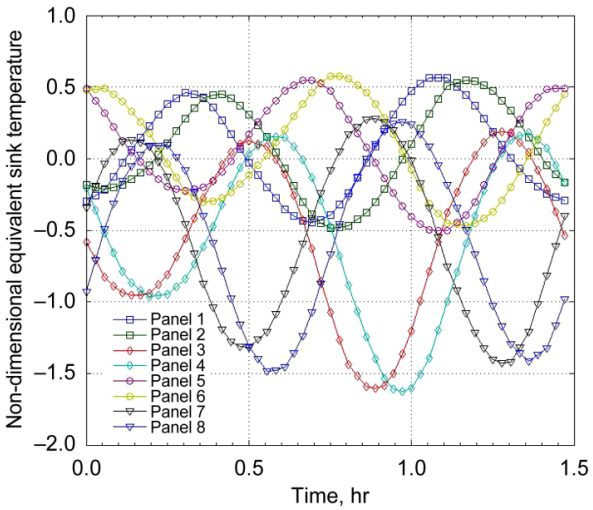



Figure 10.—Sink temperature for LEO aft-to-Sun hot case.

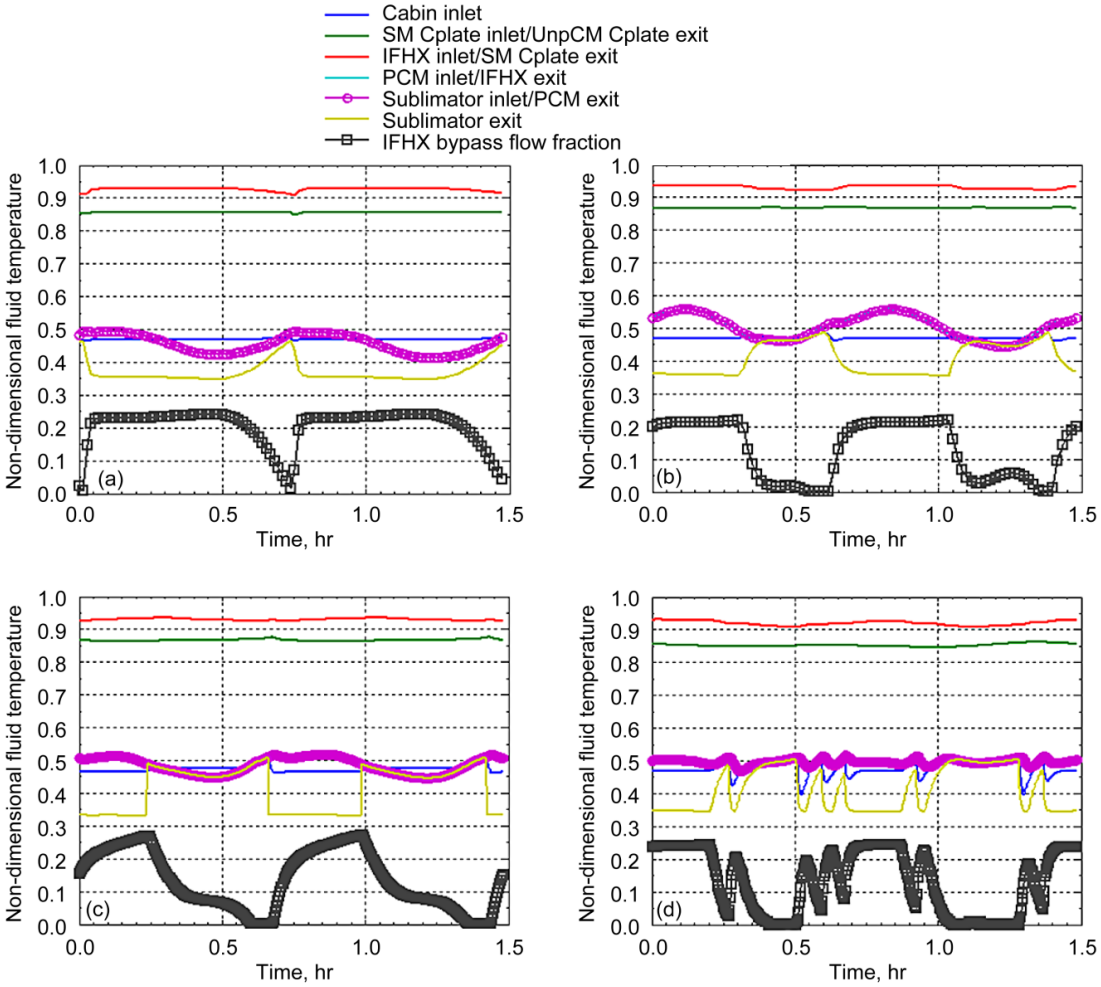



Figure 11.—Crew module (CM) fluid temperature in ATCS for LEO aft-to-Sun hot case. PCM, phase-change material. (a) Current Simulink model. (b) Independent Simulink model. (c) SINDA/FLUINT model. (d) FloCAD model.

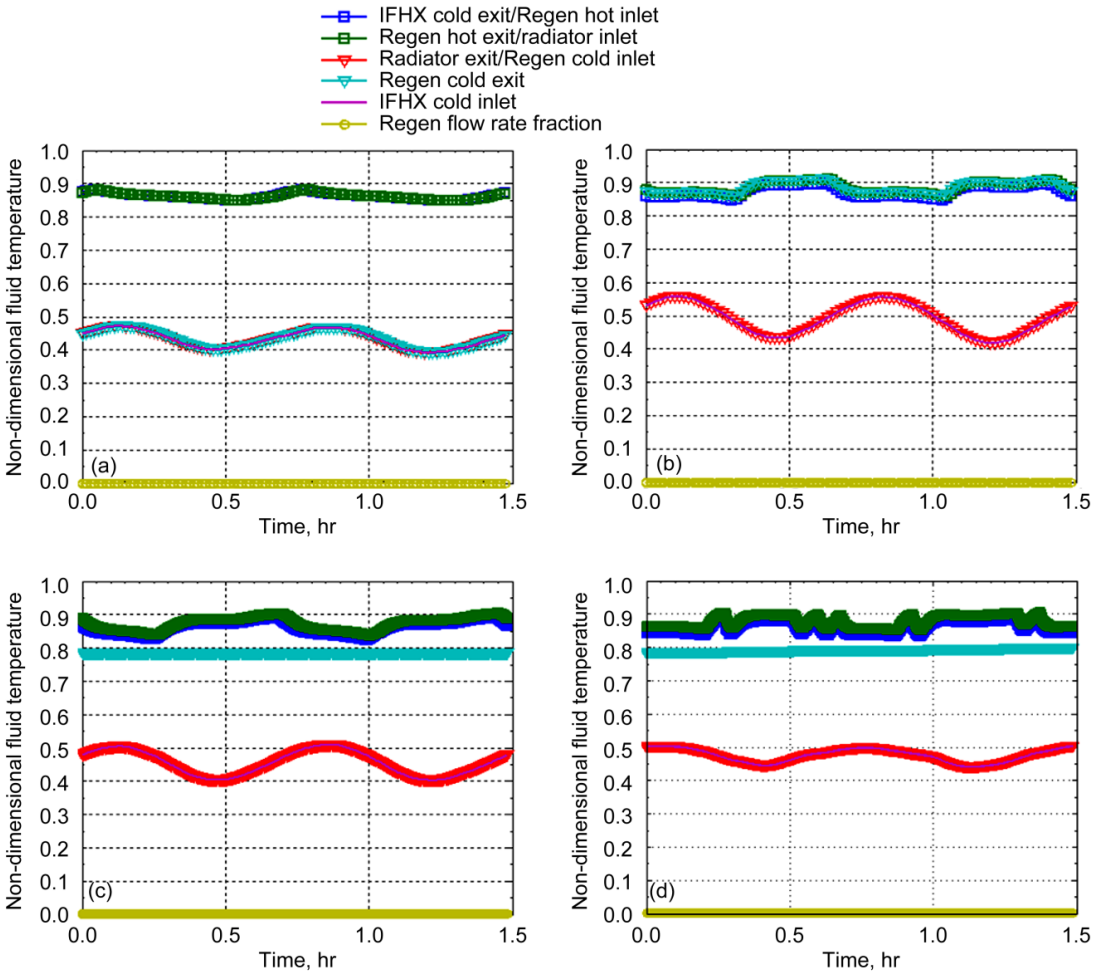



Figure 12.—Service module (SM) fluid temperature in ATCS for LEO aft-to-Sun hot case. (a) Current Simulink model. (b) Independent Simulink model. (c) SINDA/FLUINT model. (d) FloCAD model.

Figures 13 to 15 show the corresponding results for the second case. The sink temperature varied from –2.50 to 1.20. On the CM side, all models show a maximum IFHX bypass flow rate of 50 to 54 percent. On the SM side, all models show a similar pattern of Regen HX bypass flow changes. The maximum Regen HX flow rate was 40 to 65 percent. The fluid temperature drop across the radiator was similar for all the models: there was a 0.33 to 0.34 drop when the Regen HX was operating at the maximum flow rate. The difference in the Regen HX flow percentage could be due to the varying performance of the Regen HX. However, the total heat rejection should be similar for all models. When the Regen HX has no flow passing through, each model has different ways of book keeping the Regen cold exit temperatures, as shown in Figure 15. The Regen cold exit temperature is not used in the model when no flow goes through regen HX.

For the third case—a steady-state cold case—very good agreement was achieved, as shown in Figures 16 to 18. The sink temperature changed from –1.60 to –0.60. On the CM side, all models show a 68- to 69-percent IFHX bypass flow. On the SM side, the current model and SINDA/FLUINT model show 78 to 80 percent flow to the Regen HX flow, FloCAD data show 90 percent flow to the Regen HX. For all models, the temperature drop across the radiator panel was approximately 0.20.

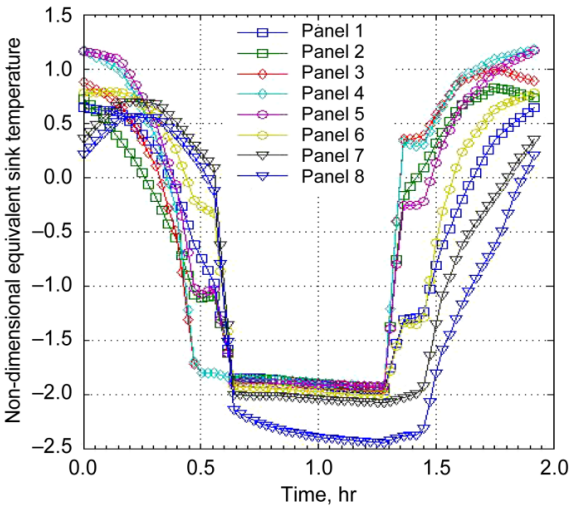



Figure 13.—Sink temperature for LLO nose-nadir hot case.

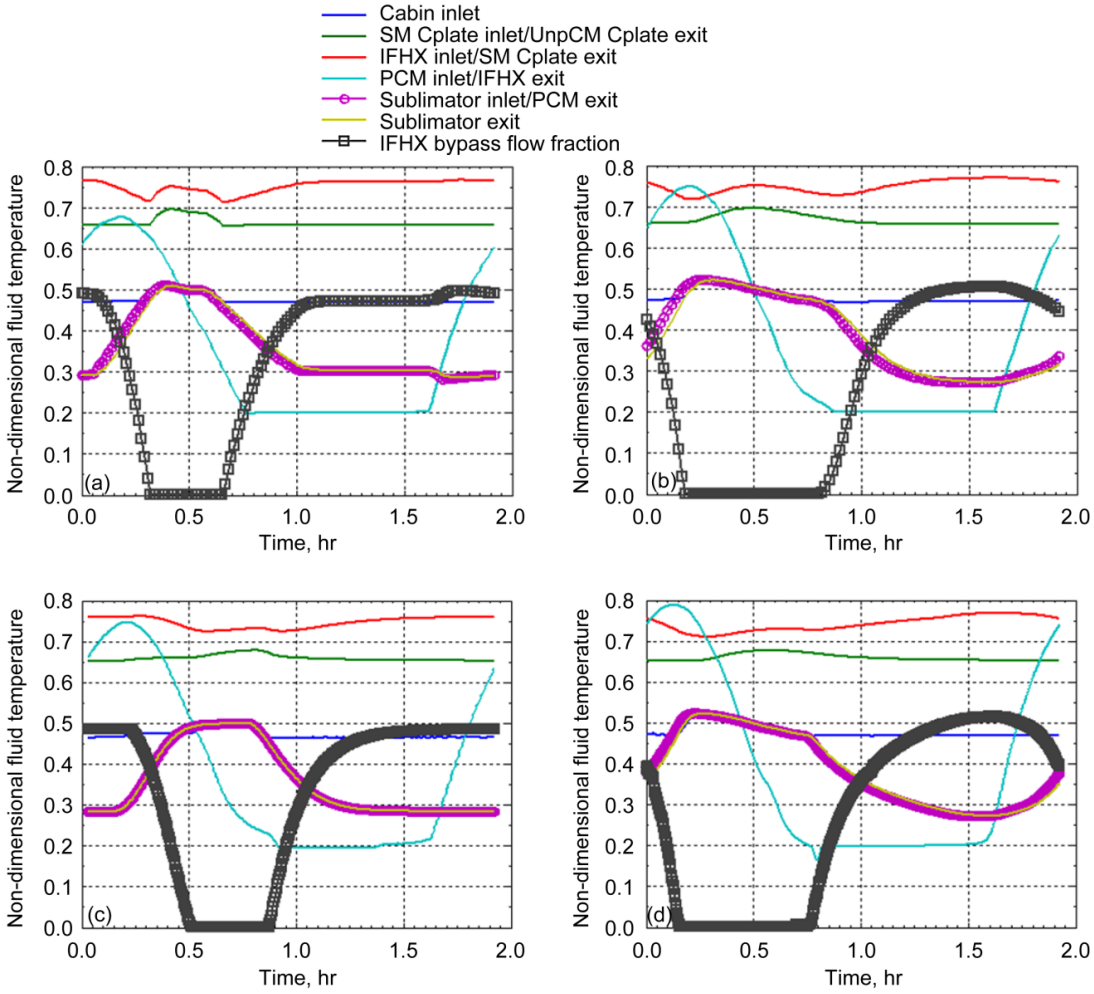



Figure 14.—CM fluid temperature in ATCS for LLO nose-nadir hot case. (a) Current Simulink model. (b) Independent Simulink model. (c) SINDA/FLUINT model. (d) FloCAD model.

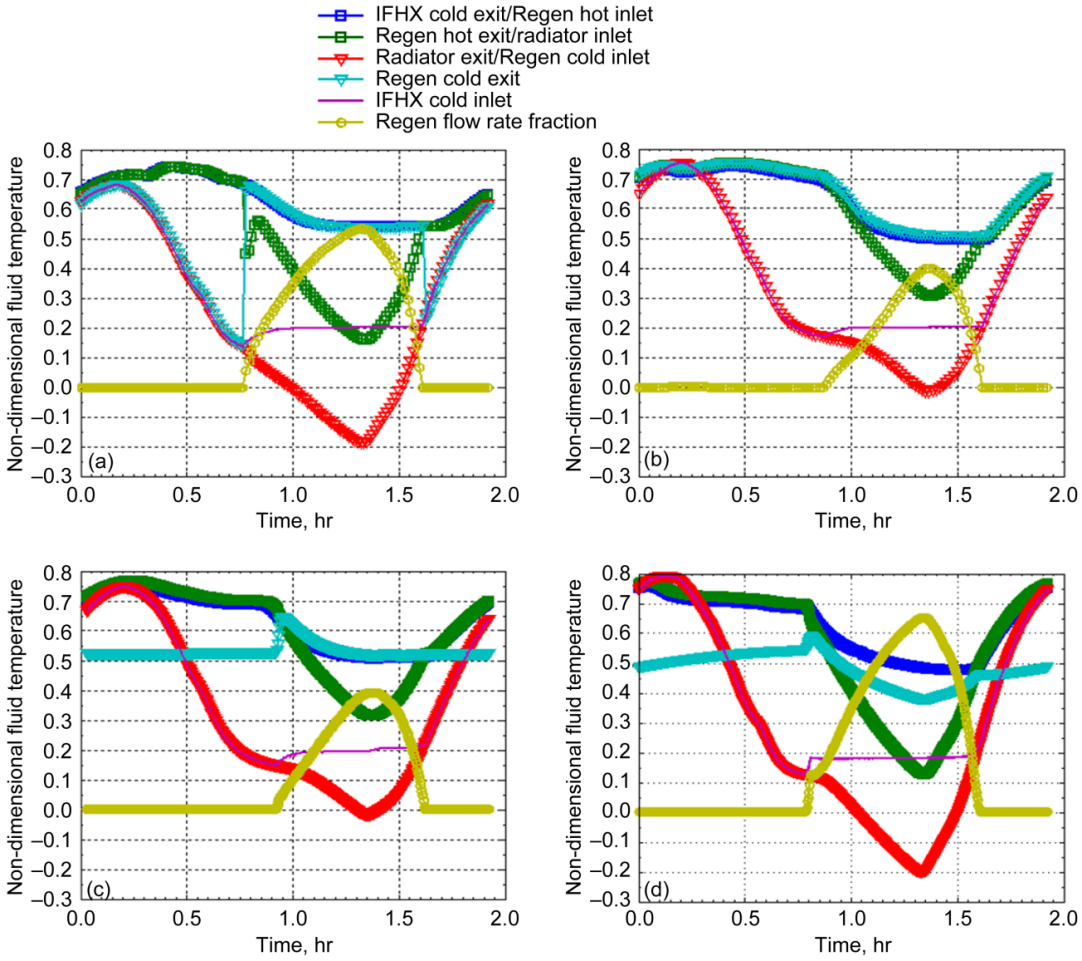



Figure 15.—SM fluid temperature in ATCS for LLO nose-nadir hot case. (a) Current Simulink model. (b) Independent Simulink model. (c) SINDA/FLUINT model. (d) FloCAD model.

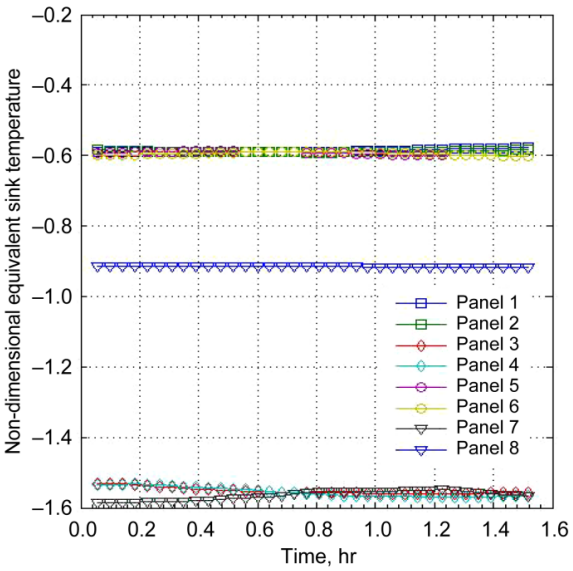



Figure 16.—Sink temperature for LLO aft-to-Sun cold case.

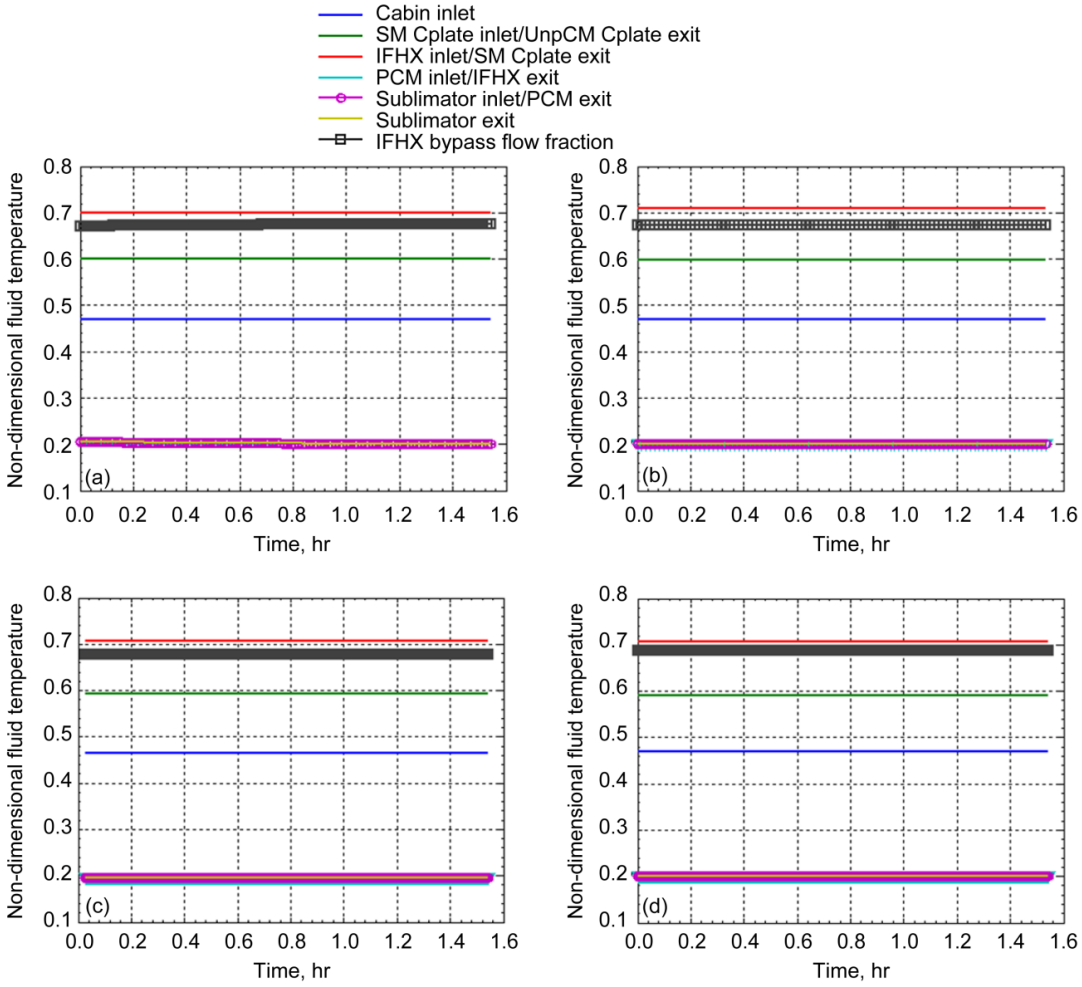



Figure 17.—CM fluid temperature in ATCS for LLO aft-to-Sun cold case. (a) Current Simulink model. (b) Independent Simulink model. (c) SINDA/FLUINT model. (d) FloCAD model.

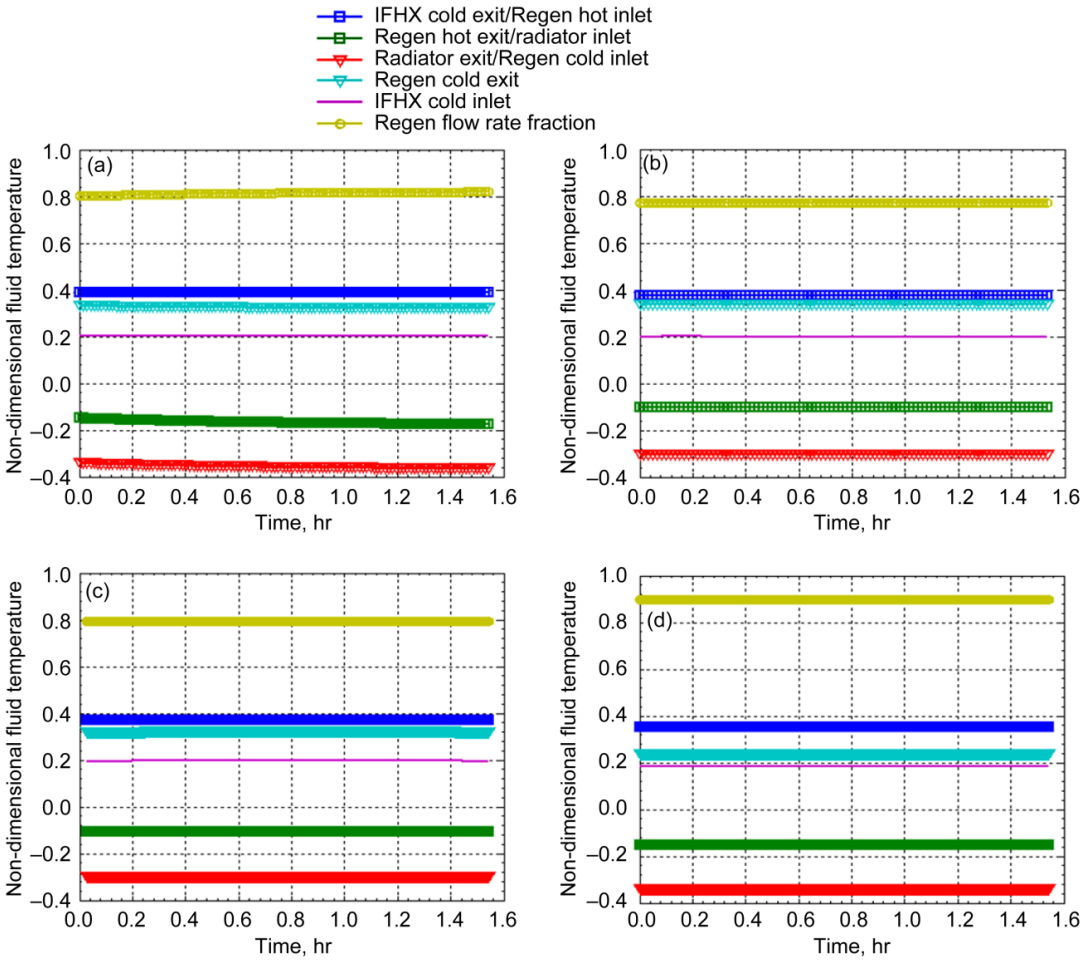



Figure 18.—SM fluid temperature in ATCS for LLO aft-to-Sun cold case. (a) Current Simulink model. (b) Independent Simulink model. (c) SINDA/FLUINT model. (d) FloCAD model.

In summary, there is reasonable agreement among the four models with the possible exception that the control algorithm in each model might be different, which would cause the transient phenomena to be slightly different, as shown in the first and second cases. All four models show simiar trends and performance for the ATCS.

## ATCS Performance for a 45-hr Nominal Mission Timeline

To further demonstrate the capability of this model, a timeline for the 45-hr nominal mission timeline was simulated to show the ATCS performance. During the mission timeline, the attitude of Orion and power loads on the ATCS vary with time. With defined attitude and power load timelines, the ATCS performance is computed and the non-dimensional fluid temperature variations on both the CM and SM sides are plotted in Figures19 and 20. The non-dimesnional heat rejection is shown in Figure 21. During the first 45 hr before docking, the ATCS was relatively “cool” compared with some hot cases studied previously. The radiator fluid inlet temperature was within 0.40 to 0.60 most of the time. The Regen HX was on most of the time, whereas the maximum regenerative flow rate was approximately 50 percent. The sublimator turned off at $t$ = 18 min and stayed off. The total sublimated water was 2.3 lbm. Note that ascent heating was not included here. The model took approximately 3 hr to simulate for the 45-hr run.

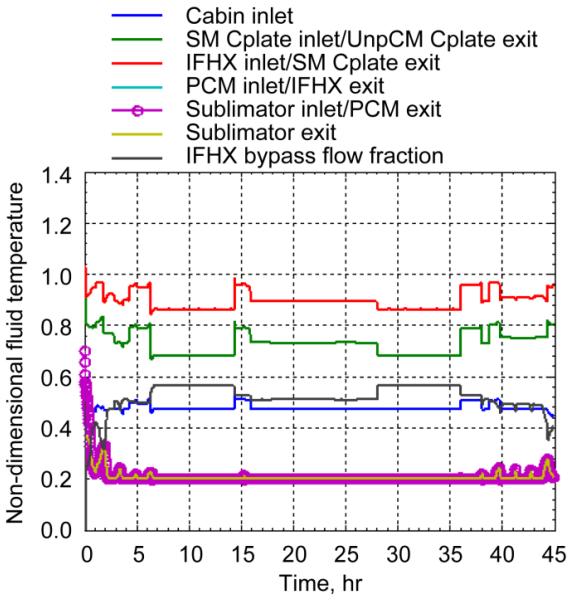



Figure 19.—Fluid temperature on CM side for 45-hr nominal mission timeline.

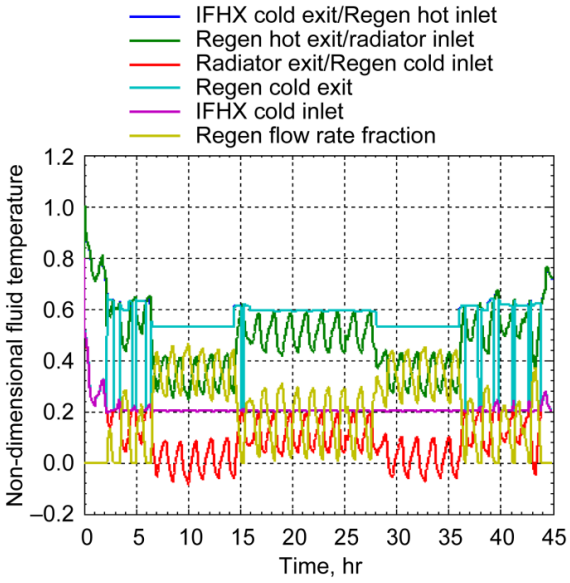



Figure 20.—Fluid temperature on SM side for 45-hr nominal mission timeline.

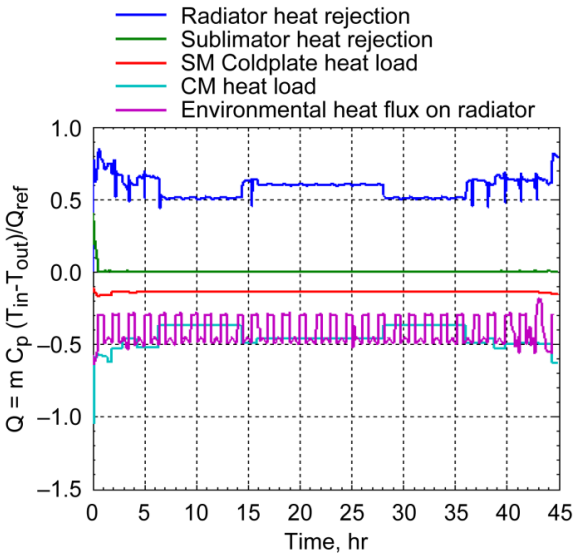



Figure 21.—Heat rejection and power load for 45-hr nominal mission timeline.

## Conclusions

A dynamic Simulink model of the *Orion* ATCS was presented. Details of the mathematical models of the heat exchanger and radiator were described. The active thermal control system model was validated using three different orbits by comparing the corresponding three results from independent resources. The agreement of the results for all four models is reasonable. All four models predict similar ATCS behavior for all three cases. Some unexplained discrepancies exist among the four models and are thought to be due to possible variations in the control algorithm used in each model. Control algorithm details were not available for this study.

## References

1. Simulink, developed by The MathWorks.
2. Thermal Desktop®, PC/CAD-based thermal model builder, developed in Cullimore & Ring (C&R) Technologies.
3. FloCAD®, PC/CAD-based thermal/fluid model builder, developed in C&R Technologies.
4. SINDA/FLUINT, a generalized thermal/fluid network-style solver.
5. NASA and Lockheed Martin Orion thermal technical interchange meeting (TIM), Dec. 2008.

| REPORT DOCUMENTATION PAGE | Form Approved OMB No. 0704-0188 |
|---|---|

The public reporting burden for this collection of information is estimated to average 1 hour per response, including the time for reviewing instructions, searching existing data sources, gathering and maintaining the data needed, and completing and reviewing the collection of information. Send comments regarding this burden estimate or any other aspect of this collection of information, including suggestions for reducing this burden, to Department of Defense, Washington Headquarters Services, Directorate for Information Operations and Reports (0704-0188), 1215 Jefferson Davis Highway, Suite 1204, Arlington, VA 22202-4302. Respondents should be aware that notwithstanding any other provision of law, no person shall be subject to any penalty for failing to comply with a collection of information if it does not display a currently valid OMB control number.
PLEASE DO NOT RETURN YOUR FORM TO THE ABOVE ADDRESS.

| 1. REPORT DATE *(DD-MM-YYYY)* | 2. REPORT TYPE | 3. DATES COVERED *(From - To)* |
|---|---|---|
| 01-05-2010 | Technical Memorandum | |

**4. TITLE AND SUBTITLE**
*Orion* Active Thermal Control System Dynamic Modeling Using Simulink/MATLAB

**5a. CONTRACT NUMBER**

**5b. GRANT NUMBER**

**5c. PROGRAM ELEMENT NUMBER**

**6. AUTHOR(S)**
Wang, Xiao-Yen, J.; Yuko, James

**5d. PROJECT NUMBER**

**5e. TASK NUMBER**

**5f. WORK UNIT NUMBER**
WBS 644423.06.32.01.03

**7. PERFORMING ORGANIZATION NAME(S) AND ADDRESS(ES)**
National Aeronautics and Space Administration
John H. Glenn Research Center at Lewis Field
Cleveland, Ohio 44135-3191

**8. PERFORMING ORGANIZATION REPORT NUMBER**
E-17146

**9. SPONSORING/MONITORING AGENCY NAME(S) AND ADDRESS(ES)**
National Aeronautics and Space Administration
Washington, DC 20546-0001

**10. SPONSORING/MONITOR'S ACRONYM(S)**
NASA

**11. SPONSORING/MONITORING REPORT NUMBER**
NASA/TM-2010-216252

**12. DISTRIBUTION/AVAILABILITY STATEMENT**
Unclassified-Unlimited
Subject Categories: 34 and 64
Available electronically at http://gltrs.grc.nasa.gov
This publication is available from the NASA Center for AeroSpace Information, 443-757-5802

**13. SUPPLEMENTARY NOTES**

**14. ABSTRACT**
This paper presents dynamic modeling of the crew exploration vehicle (Orion) active thermal control system (ATCS) using Simulink (Simulink, developed by The MathWorks). The model includes major components in ATCS, such as heat exchangers and radiator panels. The mathematical models of the heat exchanger and radiator are described first. Four different orbits were used to validate the radiator model. The current model results were compared with an independent Thermal Desktop (TD) (Thermal Desktop, PC/CAD-based thermal model builder, developed in Cullimore & Ring (C&R) Technologies) model results and showed good agreement for all orbits. In addition, the Orion ATCS performance was presented for three orbits and the current model results were compared with three sets of solutions-FloCAD (FloCAD, PC/CAD-based thermal/fluid model builder, developed in C&R Technologies) model results, SINDA/FLUINT (SINDA/FLUINT, a generalized thermal/fluid network-style solver ) model results, and independent Simulink model results. For each case, the fluid temperatures at every component on both the crew module and service module sides were plotted and compared. The overall agreement is reasonable for all orbits, with similar behavior and trends for the system. Some discrepancies exist because the control algorithm might vary from model to model. Finally, the ATCS performance for a 45-hr nominal mission timeline was simulated to demonstrate the capability of the model. The results show that the ATCS performs as expected and approximately 2.3 lb water was consumed in the sublimator within the 45 hr timeline before Orion docked at the International Space Station.

**15. SUBJECT TERMS**
Active thermal control system; Dymanic modeling; Spacecraft

| 16. SECURITY CLASSIFICATION OF: | | | 17. LIMITATION OF ABSTRACT | 18. NUMBER OF PAGES | 19a. NAME OF RESPONSIBLE PERSON |
|---|---|---|---|---|---|
| a. REPORT | b. ABSTRACT | c. THIS PAGE | | | STI Help Desk (email:help@sti.nasa.gov) |
| U | U | U | UU | 25 | 19b. TELEPHONE NUMBER *(include area code)* 443-757-5802 |